

DOI: 10.1002/cbic.200800072

Photocontrol of Single-Chain DNA Conformation in Cell-Mimicking Microcompartments

Matthieu Sollogoub,^[b] Samuel Guieu,^[b] Marie Geoffroy,^[a] Ayako Yamada,^[c] André Estévez-Torres,^[c, d] Kenichi Yoshikawa,^[c, d] and Damien Baigl^{*[a, d]}

It has been well established that the regulation of gene activity is strongly dependent on the higher-order structure of genomic DNA molecules.^[1] Several strategies have thus been developed to control the higher-order structure of long DNA molecules. Most of them have been based on the use of chemical compounds that bind to DNA to neutralize its charge, such as polyamines, multivalent metal cations, cationic surfactants, cationic polymers, nanoparticles, or crowding agents such as hydrophilic polymers.^[2] Depending on the concentration of these additives, DNA exhibits a folded or unfolded conformation. Nevertheless, with all these strategies, it is impossible to act in a reversible way on the DNA higher-order structure under a constant chemical composition.

Moreover, for transfection applications, compacting DNA is an essential step to allow the entry of DNA into the cell. In most cases, however, DNA remains in a compact conformation inside the cell, which can significantly alter the DNA gene expression. Using an external stimulus to control DNA higher-order structure within a cell-sized compartment has thus become an important challenge.

On the other hand, motivated by the perspective of DNA vectorization,^[3] preparation of artificial cells^[4] or biochemical microreactors,^[5] many scientists have attempted to encapsulate DNA into cell-like microcompartments, for example, cell-sized liposomes^[6] or phospholipid-coated microdroplets.^[7] Consequently, various successful strategies have been proposed to prepare DNA–liposome complexes^[8] or encapsulate DNA inside liposomes.^[9] In most cases encapsulated DNA molecules were typically smaller than a few thousands base pairs. However, in nature, genomic DNA molecules can be much larger, up to hundreds of kbp (kilo base pairs). To the best of our knowledge, no method has been proposed to encapsulate efficiently,

in a controlled way, and without degradation, DNA molecules that are larger than 1 kbp into cell-sized liposomes. One paper reported the encapsulation of T4 DNA molecules, but the data were not sufficient to draw conclusions about the integrity of encapsulated DNA chains.^[10] Another strategy was to encapsulate DNA in a compact state, but DNA molecules remained in their compact state once they were encapsulated.^[11]

Very recently, Le Ny and Lee made a breakthrough by proposing a system where DNA higher-structure can be controlled by light in a reversible manner.^[12] This was achieved by adding to a DNA solution a photosensitive cationic surfactant, azobenzene trimethylammonium bromide surfactant (AzoTAB). The apolar tail of the surfactant contains an azo group, which is mainly in the *trans* (more hydrophobic) conformation under visible conditions. Under UV illumination (365 nm), the azo group photoisomerizes into the *cis* (more hydrophilic) conformation. They demonstrated that there exists an AzoTAB concentration range for which DNA is in the compact state under dark/visible conditions but in the unfolded state under UV illumination, that is, DNA higher-order structure can be controlled by light. In this study, the authors mainly characterized the average property of many DNA chains in solution.

Here, we characterized the single-chain conformational behavior of long genomic DNA as a function of AzoTAB concentration and time of UV illumination. We established that the transition has a first-order character at the single-chain level. We studied the single-chain unfolding upon UV illumination and evidenced two mechanisms of single-chain DNA unfolding. Then we applied this strategy to unfold genomic DNA molecules that are encapsulated in cell-mimicking microcompartments. To this end, DNA that was compacted by AzoTAB under visible conditions was encapsulated into cell-sized microdroplets that were coated with various phospholipids prior to UV light exposition. We studied the unfolding process of individual DNA molecules inside the microdroplets. We could successfully unfold most of the DNA molecules when the phospholipid was anionic (DOPS phospholipid). We thus demonstrated how an external stimulus, here light, can be used to control the higher-order structure of individual genomic DNA molecules within cell-sized phospholipid-coated microcompartments.

By using fluorescence microscopy (FM), we characterized the conformation of individual T4 DNA molecules at a very low DNA concentration (0.1 μM) in Tris–HCl buffer (10 mM, pH 7.4). To the DNA solution, we added azobenzene trimethylammonium bromide (AzoTAB, Figure 1 A) at various concentrations under dark conditions (most of AzoTAB molecules are in the *trans* conformation, that is, more hydrophobic). Depending on AzoTAB concentration, we distinguished three regimes with re-

[a] M. Geoffroy, Dr. D. Baigl
Department of Chemistry, Ecole Normale Supérieure
24 rue Lhomond, 75005 Paris (France)
Fax: (+33) 1-4432-2402
E-mail: damien.baigl@ens.fr

[b] Prof. M. Sollogoub, S. Guieu
Institut de Chimie Moléculaire (FR2769)
Laboratoire de Chimie Organique (UMR CNRS 7611)
UPMC Université Paris 06
4, Place Jussieu, C. 181, 75005 Paris (France)

[c] Dr. A. Yamada, Dr. A. Estévez-Torres, Prof. K. Yoshikawa
Department of Physics, Kyoto University
Kitashirakawa oiwake-cho, Sakyo-ku, Kyoto 606-8502 (Japan)

[d] Dr. A. Estévez-Torres, Prof. K. Yoshikawa, Dr. D. Baigl
Spatio-Temporal Order Project, ICORP
JST (Japan Science and Technology Agency)
Kyoto University, Kyoto 606-8502 (Japan)

 A video clip is available as Supporting information on the WWW under <http://www.chembiochem.org> or from the author.

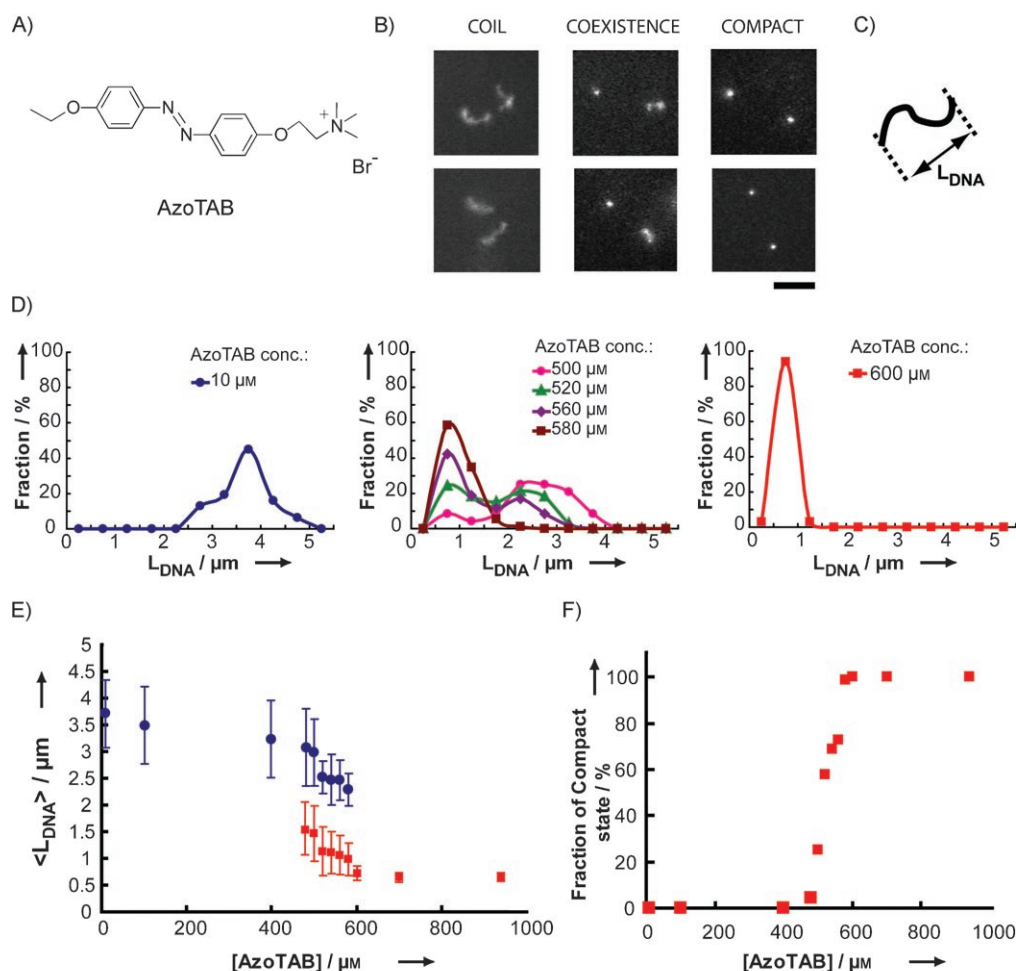


Figure 1. Phase diagram of single-chain T4 DNA in the bulk solution as a function of AzoTAB concentration. For all experiments, the T4 DNA concentration is $0.1 \mu\text{M}$ in 10 mM Tris-HCl buffer solution. A) Chemical structure of azobenzene trimethylammonium bromide (AzoTAB). B) Typical fluorescence microscopy (FM) images of T4 DNA for AzoTAB concentrations of $10 \mu\text{M}$ (left), $520 \mu\text{M}$ (middle), and $700 \mu\text{M}$ (right). Left, all DNA molecules are in the coil state. Middle, shrunk coil and compact state coexist. Right, all molecules are in the compact state. Scale bar is $5 \mu\text{m}$. C) Definition of the apparent long-axis length of single-chain DNA (L_{DNA}). D) Distributions of L_{DNA} for various AzoTAB concentrations. L_{DNA} was extracted from FM images of DNA molecules and each distribution was established on about 200 individual DNA molecules. Each point gives the fraction of DNA molecules that has a given $L_{\text{DNA}} \pm 0.25 \mu\text{m}$. Solid lines are guides. E) Average single-chain DNA size as a function of AzoTAB concentration. Blue circles correspond to molecules in the elongated or shrunk coil state, and red squares correspond to DNA molecules in the compact state. Each symbol with error bars represents the average value of L_{DNA} distributions plus or minus one standard deviation. F) Fraction of DNA molecules in the compact state as a function of AzoTAB concentration. Error bars are within the symbol size.

spect to the individual conformations of DNA molecules. For AzoTAB concentrations less than $480 \mu\text{M}$, all individual molecules were in the typical coil state, which is characterized by large intrachain fluctuations and a slow translational diffusion (Figure 1B, left). For AzoTAB concentrations greater than $580 \mu\text{M}$, we observed that all DNA molecules were in the fully compact state, which is characterized by a very fast-diffusive Brownian motion (Figure 1B, right). The diffusion coefficient of such compact DNA molecules corresponds to freely diffusing particles of approximately 100 nm in diameter, in good agreement with previously reported electron microscopy characterizations of DNA condensates.^[2b,13] For intermediate AzoTAB concentrations (between $480 \mu\text{M}$ and $580 \mu\text{M}$), fluctuating shrunk coils coexist with DNA molecules in the fully compact state (Figure 1B, middle).

For a quantitative characterization of the DNA conformational state, we measured systematically the DNA apparent long-axis length L_{DNA} (as defined in Figure 1C) of a large number of individual DNA molecules (ca. 200 per distribution) and established the distribution of L_{DNA} as a function of AzoTAB concentration (Figure 1D). Figure 1D (left) shows that at a low AzoTAB concentration, most DNA molecules are elongated ($L_{\text{DNA}} \sim 3\text{--}4 \mu\text{m}$), which is attributed to the electrostatic repulsion between phosphate groups and semiflexible nature of long DNA; the width of the distribution can be explained by the fluctuating character of individual chains due to the intrachain Brownian motion of monomers. In contrast, at a high AzoTAB concentration, the distribution is very narrow and centered around $0.7 \mu\text{m}$, which corresponds to the situation where all DNA molecules are in a very dense compact state

(Figure 1D, right). In this case, the apparent DNA long-axis length is much larger than the actual size of DNA molecules (around 100 nm), which can be explained by the blurring effect of fluorescent light.^[14] For intermediate AzoTAB concentrations, the distributions clearly indicate the coexistence of two populations: 1) a wide distribution centered on $L_{\text{DNA}} \sim 2.5 \mu\text{m}$, which corresponds to fluctuating coils but shrunk compared to the elongated coil state observed under low concentration of AzoTAB; and 2) a narrow distribution centered on $0.7\text{--}1 \mu\text{m}$ corresponding to DNA molecules in the fully compact states (Figure 1D, middle). Figure 1E shows the complete phase diagram of individual DNA molecules where the average individual DNA length that is obtained from distributions is plotted as a function of AzoTAB concentration. The coexistence region at intermediate AzoTAB concentrations is clearly evidenced. In this region, the fraction of compact state increases with an increase in AzoTAB concentration (Figure 1E). All these results show that the single-chain compaction of DNA by AzoTAB molecules is of a first-order type with the coexistence of shrunk coil and compact states at intermediate AzoTAB concentrations. Such a discrete single-chain transition is typical of DNA compaction by oppositely charged compounds, and the presence of shrunk coils in the coexistence region is more specific to a DNA–cationic surfactant interaction.^[2e] It has been interpreted theoretically as a direct consequence of the semiflexible nature of long DNA.^[15]

We studied the effect of UV light illumination on the DNA single-molecule conformation. First, DNA molecules were compacted in the presence of AzoTAB as described above. Then, we followed the evolution of single-chain DNA conformation for different UV exposure times. Figure 2A shows time–sequence fluorescence microscopy images of individual DNA molecules for two AzoTAB concentrations. At a concentration of $600 \mu\text{M}$, the DNA molecule is in the typical fully compact state before UV exposure, in agreement with the phase diagram shown in Figure 1E. With an increase in UV illumination time, the molecule expands progressively. After 50 min of UV illumination, the molecule has all the characteristics of a DNA coil (intrachain fluctuations and $L_{\text{DNA}} \sim 3 \mu\text{m}$). This unfolding process from a compact state to a (elongated or shrunk) coil upon UV illumination was observed for most DNA molecules at AzoTAB concentrations of $600 \mu\text{M}$ and $700 \mu\text{M}$. Figure 2B (left) shows the DNA size distribution as a function of UV illumination time. It confirms that the fraction of DNA molecules in the compact state decreases with an increase in illumination time, and the fraction of unfolded or partially unfolded coils increases. Figure 2C shows that this progressive unfolding upon UV illumination time is accompanied by an increase in the average size of individual DNA molecules, which seems almost independent of the AzoTAB concentration. It is interesting to compare Figures 1D and E (compaction) to Figures 2B and C (unfolding by light). During the unfolding process, the all-or-none character is less marked than during the compaction process, which might be a consequence of kinetic effects. Moreover, by considering the size distribution one notes that after compaction and UV illumination, the initial state, in which 100% of DNA molecules are in the elongated-coil state, is

never reached. After compaction and 50 min of UV illumination, all molecules are unfolded (0% of compact state) but only a small part of DNA molecules attain the elongated coiled state ($L_{\text{DNA}} \sim 3\text{--}3.5 \mu\text{m}$), and most of them reach a shrunk coil state ($L_{\text{DNA}} \sim 2.5\text{--}3 \mu\text{m}$). This might be due to a residual binding of AzoTAB molecules with DNA, which prevents DNA molecules from reaching the elongated coil state.

Furthermore, for AzoTAB concentrations higher than $800 \mu\text{M}$, we observed a different conformational response to UV illumination. At $940 \mu\text{M}$, Figure 2A (right) shows an individual DNA molecule, initially in the compact state, which also expands with an increase of UV illumination time but keeps a globular conformation. The resulting swollen globule is a highly fluctuating structure as shown in Figure 2A (AzoTAB $940 \mu\text{M}$, 50 min UV). Figures 2B and C show that all DNA molecules reach a similar conformation and never unfold regardless of UV illumination time. The characteristic fluctuations of the globule surface lead to various metastable pearling structures, and small portions of coil DNA can also be observed emerging succinctly between the “pearls”, or at the surface of the globule. This effect presents similarities with the pearl-necklace instability of polyelectrolytes under poor solvent conditions,^[16] and might be due to the competition between surface energy of the globule and electrostatic repulsion between charged monomers.^[17]

Until this point, we demonstrated how to control the bulk conformation of individual DNA molecules by light. Then, we applied this approach to DNA molecules that were encapsulated in water-in-oil phospholipid-coated microdroplets. For all experiments, a solution of DNA that was unfolded (no AzoTAB) or compacted by AzoTAB ($700 \mu\text{M}$), was encapsulated in phospholipid-coated microdroplets and exposed to UV. Under our experimental conditions, microdroplets were about $10\text{--}200 \mu\text{m}$ in diameter and contained typically $1\text{--}30$ DNA molecules. Figure 3A summarizes the results obtained under various conditions. In the absence of AzoTAB, that is, when DNA was directly encapsulated from the elongated coil state, the average size of encapsulated DNA is $1.0 \pm 0.3 \mu\text{m}$, which indicates a marked degradation of DNA chains (before encapsulation $L_{\text{DNA}} = 3.7 \pm 0.6 \mu\text{m}$); this is attributed to the strong shear stress on DNA molecules during the emulsification step. In the presence of AzoTAB ($700 \mu\text{M}$), that is, DNA was first compacted and then encapsulated, the encapsulation was carried out by using two different phospholipids: EPC and DOPS. With EPC as a phospholipid, all DNA molecules are in the compact state before UV illumination ($L_{\text{DNA}} = 0.85 \pm 0.17 \mu\text{m}$). After 22 min under UV illumination, no significant change was observed, and most of the DNA molecules remained in the compact state ($L_{\text{DNA}} = 0.82 \pm 0.14 \mu\text{m}$). Moreover, regardless of UV illumination time, a majority of observed DNA molecules were immobile or showed constrained Brownian motion in the vicinity of the droplet surfaces. All these observations indicate a strong interaction between EPC and DNA molecules. EPC is a zwitterionic phospholipid that can electrostatically interact through its cationic part with the DNA's negative phosphate groups. This can induce adsorption of DNA molecules on the phospholipid-coated droplet surface as well as favour a compact state for

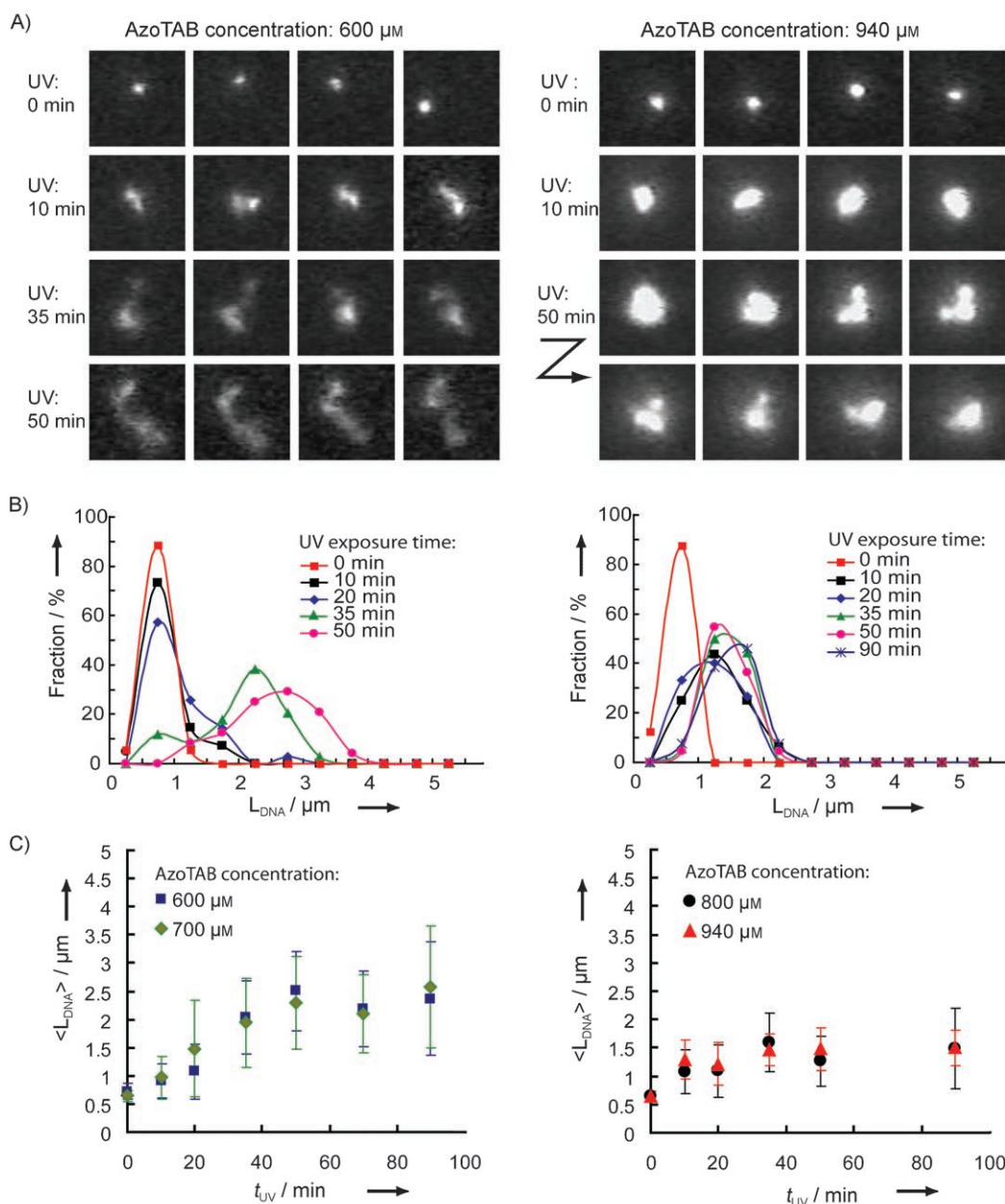


Figure 2. Single-chain DNA unfolding in bulk solution upon UV illumination. For all experiments, the T4 DNA concentration is $0.1 \mu\text{M}$ in 10 mM Tris-HCl buffer solution. A) Time-lapse sequence of fluorescence microscopy images of individual DNA molecules compacted by an AzoTAB concentration of $600 \mu\text{M}$ (left panel) and $940 \mu\text{M}$ (right panel), respectively, under UV illumination. For each panel, the pictures are separated by 100 ms along the horizontal axis, and the vertical axis corresponds to an increasing time of UV exposure (from top to bottom). The UV exposure time is indicated on the left part of each panel. Each picture has a size of $5 \times 5 \mu\text{m}$. B) Distributions of L_{DNA} (as defined in Figure 1C) as a function of UV exposure time for AzoTAB concentrations of $600 \mu\text{M}$ (left) and $940 \mu\text{M}$ (right), respectively. L_{DNA} was extracted from FM images of DNA molecules, and each distribution was established on about 200 individual DNA molecules. Each point gives the fraction of DNA molecules that have a given $L_{\text{DNA}} \pm 0.25 \mu\text{m}$. Solid lines are guides. C) Average single-chain DNA size as a function of UV exposure time for AzoTAB concentrations of $600 \mu\text{M}$ and $700 \mu\text{M}$ (left), and $800 \mu\text{M}$ and $940 \mu\text{M}$ (right). Each symbol with error bars represents the average value of L_{DNA} distributions plus or minus one standard deviation.

encapsulated DNA molecules. In contrast, when using the negatively charged phospholipid DOPS, results were markedly different. Before UV illumination, all DNA molecules were in the fully compact state, most of them diffused freely in the core of the droplets because the bare negative charge of the droplet surface prevented the DNA molecules from adsorption. Moreover, we observed the progressive unfolding of individual DNA

molecules under UV illumination. Figures 3A and B show that the average DNA length is $2.1 \pm 0.9 \mu\text{m}$ and $2.4 \pm 0.7 \mu\text{m}$ after 17 min and 32 min, respectively. DNA unfolding thus seems to be slightly faster and more efficient in the confined environment of negatively charged microdroplets than that under the bulk conditions. A precise determination of confinement effects in various microenvironments (droplets, liposomes, micro-

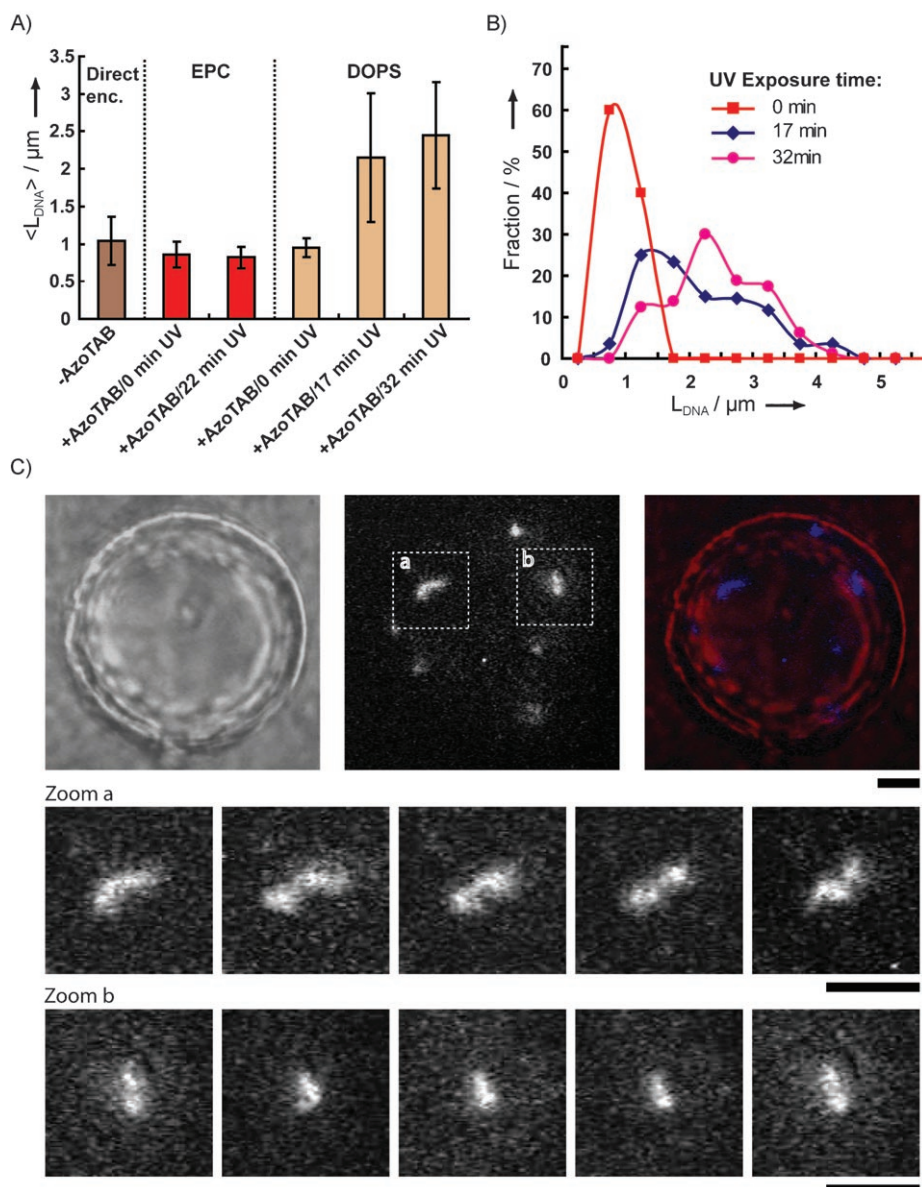


Figure 3. DNA encapsulation and unfolding by UV light inside cell-sized phospholipid microdroplets. For all experiments, a solution of T4 DNA ($0.1 \mu\text{M}$ in 10 mM Tris-HCl buffer solution), unfolded (no AzoTAB) or compacted by AzoTAB ($700 \mu\text{M}$), was encapsulated in phospholipid-coated microdroplets and exposed to different UV illumination times. A) Average DNA size for different conditions of encapsulation: without AzoTAB and with DOPS as a phospholipid (direct encapsulation); with AzoTAB, EPC as a phospholipid, and a UV illumination time of 0 or 22 min (EPC); with AzoTAB, DOPS as a phospholipid and a UV illumination time of 0, 17, or 32 min (DOPS). B) Distributions of L_{DNA} (as defined in Figure 1 C) as a function of UV exposure time. DNA molecules compacted by AzoTAB were encapsulated in microdroplets with DOPS as a phospholipid. L_{DNA} was extracted from FM images of DNA molecules and each distribution was established on about 200 individual DNA molecules. Each point gives the fraction of DNA molecules that has a given $L_{DNA} \pm 0.25 \mu\text{m}$. The solid lines are guides. C) Microscopy images of DNA that is encapsulated in a microdroplet with DOPS as a phospholipid after 32 min of UV illumination time. Top: Transmission (left), fluorescence (middle), and superposition in false colors of the transmission image (red channel) and fluorescence image (blue channel) (right). The two bottom panels show time-lapse sequences that are magnified from the zones that are indicated by the dashed squares in the upper middle picture; pictures are separated by 100 ms along the horizontal axis. All scale bars are $5 \mu\text{m}$.

DNA molecules were broken during the encapsulation, which shows that reversible compaction of long DNA molecules is a good strategy to manipulate DNA molecules under high shear forces with very few degradation. As an illustration, the movie in the Supporting Information and Figure 3C show microscopy images of unfolded DNA molecules that are encapsulated in a $28 \mu\text{m}$ DOPS-coated microdroplet after 32 min of UV illumination. In the movie, a few unfolded DNA molecules that are freely fluctuating in the droplet are clearly visible. In the images that are shown in Figure 3, two encapsulated unfolded DNA molecules are traced. The time-lapse sequences zoomed on these two molecules show that they freely fluctuate inside the droplet, and are not adsorbed on the droplet surface. All these results show that DNA molecules were encapsulated and unfolded inside the DOPS-coated microdroplets with a good yield and low degradation.

In this study, we investigated the behavior of long genomic DNA molecules (T4 DNA) in the presence of the photosensitive cationic surfactant AzoTAB in bulk and cell-mimicking microenvironments. In both cases, we showed that the conformation of individual DNA molecules can be controlled by light without changing the chemical composition of the medium. By encapsulating DNA that had been previously compacted with AzoTAB in negatively charged phospholipid-coated droplets, DNA molecules were successfully unfolded with almost no degradation inside the cell-mimicking microdroplets. Because DNA higher-order structure is strongly related to its biological activity, all

fluidic chambers) is now under investigation. One also notes that DNA molecules do not return to the initial elongated state but rather a slightly shrunk coil state, as was the case for the experiments in bulk. Finally, only a very small fraction of

these results should find applications in the development of artificial cells as well as in the control of gene expression in artificial or living environments.

Experimental Section

Materials: Phospholipids—1,2-dioleoyl-*sn*-glycero-3-[phospho-L-serine] (DOPS) and egg yolk L- α -phosphatidylcholine (EPC)—were obtained from Avanti Polar Lipids (Alabaster, USA), bacteriophage T4 DNA (166 kb) was from Wako Chemicals (Osaka, Japan), YOYO-1 iodide was from Molecular Probes. All other chemicals were purchased from Sigma. Deionized water (Millipore, 18 MOhm cm⁻¹) was used for all experiments.

AzoTAB synthesis: Azobenzene trimethylammonium bromide (AzoTAB) synthesis was adapted from the method that was described by Hayashita et al.^[18] The purity of the final product was checked by 250 MHz ¹H and ¹³C NMR spectroscopy.

Preparation of DNA samples: Water, Tris-HCl buffer, YOYO-1 iodide, and AzoTAB were mixed in this order prior to careful T4 DNA introduction (under low-shear conditions to avoid DNA breakage). For all experiments, we used T4 DNA at a final concentration of 0.1 μ M (concentration in nucleotides) in Tris-HCl buffer (10 mM, pH 7.4) with YOYO (0.01 μ M) as a DNA fluorescent dye. Under these conditions, it has been established that T4 DNA molecules essentially do not interact with each other (dilute regime). Final AzoTAB concentrations were between 0 and 1 mM. For all steps except UV illuminations, DNA samples were kept under dark conditions. Samples were equilibrated during 15 min prior to DNA characterization by fluorescence microscopy. All experiments were performed at ambient temperature.

DNA encapsulation in phospholipid-coated microdroplets: The detailed method of microdroplet preparation is described in ref. [7]. Briefly, a phospholipid film (EPC or DOPS) was prepared by evaporating a chloroform solution that contained the phospholipids under nitrogen flow. After drying for 1 h under vacuum, the film was dissolved in mineral oil under sonication at 50 °C for 1 h. Right after sonication, phospholipid solution in oil was vortexed for approximately 2 min and used within one day. The final concentration of phospholipid in oil was 0.5 mM for all experiments. DNA encapsulation was achieved by pipetting the DNA sample solution (4 μ L) up and down into oil that contained phospholipids (200 μ L) for approximately 1 min.

UV illumination: UV exposure was performed by placing the sample (DNA solution or emulsion of microdroplets that contained DNA) at 6–8 cm distance from an 8 W UVLMS-38 UV lamp (UVP, Upland, CA, USA) at 365 nm.

Fluorescence microscopy: Fluorescence microscopy was performed on an Axiovert 135 inverted microscope (Carl Zeiss), equipped with a 100 \times oil-immersed objective lens. Images were acquired by using an EB-CCD camera and an image processor Argus 10 (Hamamatsu Photonics, Hamamatsu, Japan). For characterization of DNA conformation in bulk solution, DNA samples were introduced in custom-built observation cells, where the observation area consisted of two cover glass slides separated by about 150 μ m. For characterization of DNA conformation inside microdroplets, the emulsion that contained microdroplets was introduced into a chamber that was made of a PDMS (polydimethylsiloxane/RTV615 in a 1:10 ratio, General Electrics) slab stuck on a cover glass slide, which was previously treated by trimethylchlorosilane in the vapor phase to make it hydrophobic and avoid droplet spreading.^[7] For all experiments, glass slides were previously cleaned by baking at 500 °C for 1 h.

Keywords: biomimetism • DNA • liposomes • photocontrol • self-organization

- [1] a) B. Dorigo, T. Schalch, A. Kylanara, S. Duda, R. R. Schroeder, T. J. Richmond, *Science* **2004**, *306*, 1571–1573; b) N. J. Francis, R. E. Kingston, C. L. Woodcock, *Science* **2004**, *306*, 1574–1577.
- [2] a) V. A. Bloomfield, *Curr. Opin. Struct. Biol.* **1996**, *6*, 334–341; b) L. C. Gosule, J. A. Schellman, *Nature* **1976**, *259*, 333–335; c) A. A. Zinchenko, K. Yoshikawa, D. Baigl, *Adv. Mater.* **2005**, *17*, 2820–2823; d) J. Widom, R. L. Baldwin, *Biopolymers* **1983**, *22*, 1595–1620; e) S. M. Mel'nikov, V. G. Sergeev, K. Yoshikawa, *J. Am. Chem. Soc.* **1995**, *117*, 2401–2408; f) W.-H. Huang, A. A. Zinchenko, C. Pawlak, Y. Chen, D. Baigl, *ChemBioChem* **2007**, *8*, 1771–1774; g) A. A. Zinchenko, K. Yoshikawa, D. Baigl, *Phys. Rev. Lett.* **2005**, *95*, 228101; h) A. A. Zinchenko, T. Sakae, S. Araki, K. Yoshikawa, D. Baigl, *J. Phys. Chem. B* **2007**, *111*, 3019–3031; i) U. K. Laemmli, *Proc. Natl. Acad. Sci. USA* **1975**, *72*, 4288–4292.
- [3] D. D. Lasic, *Liposomes in Gene Delivery*, CRC Press, Boca Raton, **1987**.
- [4] a) V. Noireaux, A. Libchaber, *Proc. Natl. Acad. Sci. USA* **2004**, *101*, 17669–17694; b) I. A. Chen, K. Salehi-Ashtiani, J. W. Szostak, *J. Am. Chem. Soc.* **2005**, *127*, 13213–13219.
- [5] a) A. Karlsson, R. Karlsson, M. Karlsson, A. S. Cans, A. Stromberg, F. Ryttsen, O. Orwar, *Nature* **2001**, *409*, 150–152; b) D. S. Tawfik, A. D. Griffiths, *Nat. Biotechnol.* **1998**, *16*, 652–656; c) A. D. Griffiths, D. S. Tawfik, *EMBO J.* **2003**, *22*, 24–35; d) A. V. Pietrini, P. L. Luisi, *ChemBioChem* **2004**, *5*, 1055–1062.
- [6] *Giant Vesicles: Perspectives in Supramolecular Chemistry* (Eds.: P. L. Luisi, P. Walde), Wiley, Chichester, **2000**.
- [7] a) A. Yamada, Y. Yamanaka, T. Hamada, M. Hase, K. Yoshikawa, D. Baigl, *Langmuir* **2006**, *22*, 9824–9828; b) M. Hase, A. Yamada, T. Hamada, D. Baigl, K. Yoshikawa, *Langmuir* **2007**, *23*, 348–352.
- [8] a) H. Gershon, R. Ghirlando, S. B. Guttman, A. Minsky, *Biochemistry* **1993**, *32*, 7143–7151; b) V. P. Torchilin, T. S. Levchenko, R. Rammohan, N. Volodina, B. Papahadjopoulos-Sternberg, G. G. M. D'Souza, *Proc. Natl. Acad. Sci. USA* **2003**, *100*, 1972–1977; c) H. Liang, D. Harries, G. C. L. Wong, *Proc. Natl. Acad. Sci. USA* **2005**, *102*, 11173–11178.
- [9] a) G. J. Dimitriadis, *Nucleic Acids Res.* **1979**, *6*, 2697–2705; b) R. T. Fraley, C. S. Fornari, S. Kaplan, *Proc. Natl. Acad. Sci. USA* **1979**, *76*, 3348–3352; c) M. I. Angelova, N. Hristova, I. Tsoneva, *Eur. Biophys. J.* **1999**, *28*, 142–150; d) E. Boukobza, A. Sonnenfeld, G. Haran, *J. Phys. Chem. B* **2001**, *105*, 12165–12170.
- [10] S.-i. M. Nomura, Y. Yoshikawa, K. Yoshikawa, O. Dannenmuller, S. Chaserot-Golaz, G. Ourisson, Y. Nakatani, *ChemBioChem* **2001**, *2*, 457–459.
- [11] M. Le Berre, M.-A. Guedeau-Boudeville, Y. Chen, D. Baigl, *Proc. microTAS 2006* **2006**, *2*, 1399–1401.
- [12] A.-L. M. Le Ny, C. T. Lee Jr, *J. Am. Chem. Soc.* **2006**, *128*, 6400–6408.
- [13] a) N. V. Hud, K. H. Downing, *Proc. Natl. Acad. Sci. USA* **2001**, *98*, 14925–14930; b) C. C. Conwell, I. D. Vilfan, N. V. Hud, *Proc. Natl. Acad. Sci. USA* **2003**, *100*, 9296–9301; c) D. Baigl, K. Yoshikawa, *Biophys. J.* **2005**, *88*, 3486–3493.
- [14] K. Yoshikawa, Y. Matsuzawa, *Phys. D* **1995**, *84*, 220–227.
- [15] K. Yoshikawa, M. Takahashi, V. V. Vasilevska, A. R. Khokhlov, *Phys. Rev. Lett.* **1996**, *76*, 3029–3031.
- [16] a) A. V. Dobrynin, M. Rubinstein, S. P. Obukhov, *Macromolecules* **1996**, *29*, 2974–2979; b) A. Kiriy, G. Gorodyska, S. Minko, W. Jaeger, P. Štěpánek, M. Stamm, *J. Am. Chem. Soc.* **2002**, *124*, 13454–13462; c) D. Baigl, M. Sferazza, C. E. Williams, *Europhys. Lett.* **2003**, *62*, 110–116; d) D. Baigl, R. Ober, D. Qu, A. Fery, C. E. Williams, *Europhys. Lett.* **2003**, *62*, 588–594.
- [17] a) J. W. S. Rayleigh, *Philos. Mag.* **1882**, *14*, 184–186; b) Y. Kantor, M. Kardar, *Europhys. Lett.* **1994**, *27*, 643–648.
- [18] T. Hayashita, T. Kurosawa, T. Miyata, K. Tanaka, M. Igawa, *Colloid Polym. Sci.* **1994**, *272*, 1611–1619.

Received: January 31, 2008

Published online on April 11, 2008